Heliyon 9 (2023) e21623

Contents lists available at ScienceDirect

Heliyon

journal homepage: www.cell.com/heliyon

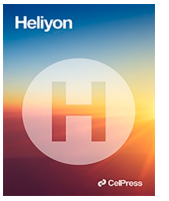

Occupational safety assessment of biogenic urea nanofertilisers using *in vitro* pulmonary, and *in vivo* ocular models

Ayushi Priyam [a,b], Prerna Seth [a], Jibananda Mishra [c], Palash Kumar Manna [a], Pushplata Prasad Singh [a,*]

[a] *National Centre of Excellence for Advanced Research in Agricultural Nanotechnology, TERI - Deakin Nanobiotechnology Centre, Sustainable Agriculture Division, The Energy and Resources Institute (TERI), New Delhi, 110003, India*
[b] *IMPACT, School of Medicine, Deakin University, Geelong, Victoria, 3217, Australia*
[c] *AAL Biosciences Research Pvt. Ltd., Panchkula, Haryana, 134109, India*

ARTICLE INFO

Keywords:
Urea
Nanofertilisers
Biological synthesis
Dermal effects
Pulmonary effects
Ocular effects

ABSTRACT

Nanomaterials (NMs) are now gaining popularity to be used in agriculture as fertilisers to reduce the dose of conventional fertilisers and enhance nutrient use efficiency. Urea has found its application as a conventional nitrogenous fertiliser since long, however, the nutrient use efficiency of the bulk form of urea is low due to issues related to ammonia volatilisation. This study proposes a biogenic synthesis route to develop urea nanoparticles that can be used as nano-fertiliser for better uptake and hence improved nutrient efficiency. Large scale production and widespread application of these nano-fertilisers to the agricultural fields will enhance the direct exposure to workers and farmers. Therefore, the occupational safety evaluation becomes critical. In this study, we report a new method for synthesis of urea nanoparticles (TNU, absolute size: 12.14 ± 7.79 nm) followed by nano-safety evaluation. Herein, the pulmonary and ocular compatibilities of TNU were investigated *in vitro* and *in vivo* respectively. The assay for cellular mitochondrial activity was carried out on human lung fibroblasts (WI-38) under varied TNU exposure concentrations up to 72 h. The acute biocompatibility effect, ocular irritation and sub-lethal effects were measured on New Zealand Rabbit. The results show that TNU do not exhibit any cytotoxicity and detrimental cell mitochondrial activity up to the highest tested concentration of 1000 μg/mL and 72 h of testing. The animal experiment results also show that neither acute nor sub-lethal toxic effects can be detected after TNU ocular instillation up to 21 days when tested up to environmentally relevant concentration of 15 μg/mL. These results suggest the occupational safety of biogenic urea nanoparticles and support its application as nanofertiliser.

1. Introduction

Use of nanomaterials (NMs) for agricultural applications has grown rapidly over the last decade [1]. There is great progression in development of new NMs to replace the conventional fertiliser doses, especially, to address low nutrient use efficiency of macronutrients such as phosphorus, nitrogen, and potassium and their poor-availability in soil [2,3]. Presently, urea is used for nitrogen supplementation across the globe. However, major challenges with urea fertilisers are associated with its' low nutrient use efficiency

* Corresponding author.
E-mail address: pushplata.singh@teri.res.in (P.P. Singh).

https://doi.org/10.1016/j.heliyon.2023.e21623
Received 14 July 2023; Received in revised form 11 October 2023; Accepted 25 October 2023
Available online 28 October 2023

(~30–50 %), insoluble nitrate formation in soils, ammonia volatilisation, and extensive leaching (~50–70 %) [4]. Urea leaching also has side effects on soil biota and the environment. The use of NMs as fertilisers and pesticides has shown promising results in terms of increased nutrient use efficiency, enhanced plant productivity, decreased usage of chemical fertilisers, mitigation of undesirable effects of agricultural practices on soil and water, and benefit to the farmers economically [5–7]. In 2021, the Indian Farmers Fertiliser Cooperative (IFFCO) using nanotechnology, have developed and commercialised Nanourea to improve nitrogen use efficiency [8,9]. In another report by Singh et al. (2023), biogenically synthesised urea based NMs have been reported to show efficacy as nitrogen supplementing nanofertiliser [10].

Biosynthesis [11] and green solvent free synthesis [12] has been suggested as one of the sustainable approaches for large scale production of nanoparticles. Use of microorganisms such as bacteria enables both intracellular and extracellular synthesis of nanoparticles as a bacterial flux response to addition of substrate [11]. Intracellular process recovers metals from biomining and it has been reported that bio-mined metallic nanoparticles can also act as catalysts in different other chemical reactions [13]. The extracellular process uses the reductive components of cell wall to reduce the ions from the substrate [11]. Most recent reports during 2022–2023 include the synthesis of silver [14,15], zinc-oxide [16] and copper [17] nanoparticles using microorganisms. However, there are only few reports where nanoparticles intended for agricultural purposes have been synthesised using micro-organisms due to microbial metabolic responses [18–20].

The release of nanoparticles and workplace exposure is expected to increase as these nitrogen-supplementing nanofertilisers are synthesised and used more widely. Therefore, it is also important to analyse the safety of the new nanofertilisers using suitable model systems to identify any potential occupational risk at the workplace. The reports on biocompatibility evaluation of NMs containing urea as one of the components are very few with no reports on occupational toxicity evaluation of urea nanoparticles intended for agricultural applications. However, there are few reports where biocompatibility is evaluated for heterogenous NMs in which urea has been used as one of the components. Previously a study by Hasanzadeh et al. (2021) has reported the biocompatibility of silver nanoparticles synthesised onto the urea-based periodic mesoporous organosilica in NIH-3T3 cells [21]. Another study by Adewuyi et al. (2022) has reported biocompatibility of urea imprinted cobalt ferrite nanoparticles in albino rats [22]. On contrary another study by Ghasempour et al. (2014) has reported toxicity of urea coated ferrous oxide nanoparticles on L929 cell line [23].

The guidelines for safety assessment of manufactured nano-agri-inputs and nano-agri-products from Department of Biotechnology, India [24] has recommended several test guidelines from Organisation for Economic Co-operation and Development (OECD) to assess occupational safety from the agriculturally relevant NMs [24]. Among various parameters, test guidelines for eye irritation and inhalation toxicity are included for the occupational safety of the agriculturally relevant NMs [24]. Human cell lines such as alveolar basal epithelial cells (A549), bronchial epithelial cells (Beas2B) and lung fibroblast cells (WI-38) have been used in several studies to define the *in vitro* pulmonary effects and inhalation toxicity of NMs. Analysis the reports between 2019 and 2023 for *in vitro* pulmonary toxicity, shows that NMs such as crystalline silica [25], graphene oxide [26], zinc oxide [26], silver [27] and copper oxide [28] nanoparticles cause toxicity on A549 cells. Several other studies have also reported toxicity of nano-biochar [29], nano copper oxide [30,31], nano size coal dust [32], nano-Nickel [33] and graphene oxide composites [34] on Beas2B cells. These studies have limited discussions on the occupational or environmentally relevant doses of the tested NMs. Similarly, nanotoxicity reports in WI-38 are also restricted to the dose-dependent studies of cellulose-zinc oxide-silver nanocomposites [35], silica nanoparticles [36] and biogenic silver nanoparticles [37]. It is therefore an open area to explore the *in vitro* effects of the new manufactured NMs on lung fibroblasts (WI-38) as they are essential to maintain the alveolar structural integrity when subjected to external stress [38].

OECD test guideline 405 suggests the assessment of acute eye irritation/corrosion as a measure of potential health hazard that may occur due to exposure to different types of liquids/aerosols [39]. Ocular toxicity of NMs by following the OECD test guideline 405 and using rabbit model has been reported in a very few studies that involved cationic solid lipid nanoparticles [40], graphene oxide [41,42] and magnetic nanoparticles [43]. However, the safety assessment for agriculturally useful NMs such as those based on urea-based nanoparticles has not been reported for the health risks associated with their ocular exposure before their applications.

In the present study, for the first time, we report biogenic synthesis of urea nanoparticles (TNU) and their safety evaluation by using *in vitro* cell line human lung fibroblasts (WI-38) and an *in vivo* New Zealand rabbit model for acute and sub-lethal ocular toxicity at doses relevant to environmental application and occupational hazard. The use of biosynthesis approach to develop urea nanoparticles is hypothesised to reduce the carbon footprint of the fertiliser development process due to following major factors: i. the single step bio-reduction process requires lesser energy as compared to synthesis of conventional chemical fertilisers and ii. the components used for synthesis come from microorganisms instead of corrosive acids or alkalis resulting in zero toxic by-products. Additionally, the trial application of urea nanoparticles to fields have demonstrated that their use can reduce the requirement of conventional urea fertilisers [8–10], resulting in lowering the overall burden of fertilisers on the environment. The study is very relevant in the present times when to enhance agriculture productivity in a sustainable manner is most desirable.

2. Materials and methods

2.1. Materials

Technical Urea (non-nano) was procured from Zuari Agro Chemicals Limited. Nutrient broth and agar were procured from HiMedia. The reagents used in this study were of high purity and were used without any further purification. Milli-Q water was used to prepare all the solutions. Fetal Bovine Serum (FBS) and DMEM was purchased from Gibco (Massachusetts, USA). Heat inactivated FBS was added to the DMEM media after filter sterilisation. The proteins were used without further purification. Autoclaved, sterile water (Millipore, Milli-Q water with a conductivity of 18.2 MΩ cm) was used wherever required.

2.2. Biogenic synthesis and physicochemical characterisation of urea nanoparticles (TNU)

By using technical urea as a substrate, a novel formulation containing nanoparticles of urea (TNU) was synthesised using a consortium of two *Bacillus* species via fermentation technology. The *Bacillus* species were procured from the germplasm collection at TDNBC, TERI, Gwal Pahari, Gurugram, India. Characterisation of TNU was done following the NIST (NCL) protocols. Hydrodynamic size distribution, polydispersity index, and zeta potential of the synthesised particles were evaluated using Zetasizer Nano-ZS (Malvern Instruments, UK) [44]. Further actual particle size was evaluated using TEM (Tecnai G2 30-U twin microscope, FEI, USA) at a voltage of 200 kV [45]. The crystal structure of TNU was identified with a Rigaku X-ray diffractometer using CuKα radiation (1.5404 Å) at 15 mA and 40 kV. The spectrum was recorded at 2θ ranging from 3° to 70° with a scanning step of 0.01° per second. The crystallite size was directly obtained from the instrument readings based on the Debye-Scherrer equation. The FTIR spectra was recorded by using Thermofisher FTIR Spectrum™ to detect the functional groups present in the sample via ATR mode in the frequency range of 400–4000 cm^{-1}. Raman spectra was recorded using in the range of 98–6111 cm^{-1} at 532 nm using an EnSpectr R532 Raman analyser. Hydrodynamic parameters were also characterised in the *in vitro* cell culture media with and without serum where the characteristics of TNU in de-ionised (DI) water were considered as control for comparisons.

2.3. In vitro effects of biogenic urea nanoparticles in WI-38 cells

The *in vitro* effects of the TNU were determined by using human lung fibroblast cells (WI-38). Commercially available WI-38 cells from ATCC, US were grown in DMEM supplemented with 10 % (*v/v*) FBS and 1 % (*v/v*) penicillin-streptomycin at 37 °C. The cell viability on account of superoxide dismutase activity was determined by WST-1 assay by following the previously published protocols [46]. Briefly, the cells were seeded in a 96-well plate at a seeding density of 10^4 cells per well in 100 μL serum supplemented media. At 80 % confluence, the cells were exposed to the TNU at increasing concentrations of 1.5, 2.5, 3.1, 5, 6.25, 7.5, 10, 12.5, 25, 50, 100, 250, 500, and 1000 μg/mL relevant to environmentally relevant and supra-environmentally relevant concentrations [47,48]. The untreated cells (0 μg/mL of TNU) were considered as control. After incubation at 24, 48 and 72 h from the exposure, 10 μL of WST-1 reagent was added to each well. The cells were incubated for 4h at 37 °C and 5 % CO_2. The cellular activity by measuring absorbance at 490 nm with reference to the untreated control.

2.4. Animal ethics statement

All the experiments on the New Zealand rabbits were approved by the Institutional Animals Ethics Committee (IAEC). The IAEC Approval No for this study was MMCP-IAEC-140.

2.5. Animals, housing conditions and treatments

Two months old, female New Zealand rabbits were grouped in different treatment categories (untreated control, saline 0.9 % *w/v* and three different doses of test substance) with three individuals in each group per replicate. Therefore, a total of five groups with three replicates were used for the experiments. The animals were individually housed under standard temperature (23 °C–25 °C) and relative humidity (60 %–70 %) conditions with a 12:12 h light–dark cycle. The animals were fed and given water *ad libitum* throughout the experimental period. Treatment samples *viz.* saline 0.9 % (*w/v*) and TNU at the doses 3.75, 7.5 and 15 μg/mL were in liquid form. Instillation of each dose of the samples was done on one eye using a fresh and sterile dropper.

2.6. Acute effects of biogenic urea based nanofertilisers in New Zealand rabbits

The acute effects of TNU on the New Zealand rabbits were determined by survival and monitoring the toxic responses to different dose levels including clinical observations, sensory activities, grip strength and motor activities up to 21 days from treatments (3.75, 7.5 and 15 μg/mL). Three animals per treatment were investigated.

2.7. Ocular and sub-lethal effects of biogenic urea based nanofertilisers in New Zealand rabbits

Ocular lesions were graded, and bodyweights were measured up to 21 days from treatments. According to OECD test guideline 405 [39], lesions were graded in cornea, iris, conjunctivae and for chemosis depending upon degree of density. In cornea, the grading was done from 0 to 4 depending on the opacity with no opacity graded as 0 and opaque cornea graded as 4. In iris, the grading (0–2) was done for normal (as 0) and haemorrhage/gross destruction/no reaction to light (as 2). In conjunctivae, grading (0–3) was done as 0 for normal and 3 for diffuse beefy red. For chemosis, the grading was done from 0 to 4 for 0 being graded to normal eyes and 4 to swelling with lids more than half closed.

2.8. Statistical analyses

GraphPad Prism (v9.5) was used for statistical analyses. In a typical experiment, all values were expressed as the mean ± standard deviation (S.D.) of samples. We investigated dose-effect correlations for TNU. Shapiro-Wilk test was used to determine whether the data had a normal distribution, and QQ-plots were used to determine whether residuals had a normal distribution. ANOVA was used to

determine whether the *in vitro* and *in vivo* effects were significant with reference to the untreated control. A Tukey post hoc multiple comparison test was used to determine the treatment groups with significant differences in mean values because this would not explicitly indicate where the major differences reside. Statistical significance was defined at a p-value<0.05.

3. Results and discussion

3.1. Characterisation of biogenic urea nanoparticles (TNU)

TNU were biogenically synthesised by exposing a co-culture of two strains of *Bacillus* species for 24 h with 20–30 % technical urea as substrate. Microorganisms has been previously reported to aid the synthesis of nanoparticles [18–20]. Previously, Bahrulolum et al. (2021) have reviewed the microorganisms mediated synthesis of metallic nanoparticles to be used in agriculture [49]. The nano-synthesis associated parameters for TNU are provided in **ESI Figs. 1–3**.

Spectral characterisation of TNU was done using a UV–Vis spectrophotometer (Fig. 1a.). Two absorption peaks were noted at 210 and 265 nm, on account of a carbonyl group (C═O) present. The peak at a longer wavelength of 265 nm is a result of n→π* transition, whereas the absorption peak at 210 nm can be attributed to π→π* transition. Substituting –NH_2, an electron-withdrawing group on the carbonyl produces a hypochromic shift of the n→π* transition band, usually observed in the 280–290 nm range, and a lesser bathochromic effect on the π→π* transition, commonly observed at 190 nm [50]. The UV–Vis spectrum for the bulk urea shows differences as compared to the nanoparticles and is presented in ESI Fig. 4b.

Synthesised TNU was also analysed using Fourier transformed infrared and Raman spectroscopy. The FTIR spectrum displays characteristic peaks associated with urea (Fig. 1b.). Three prominent peaks at 3250, 1640, and 1030 cm^{-1} were observed. The broad peak at 3250 cm^{-1} is assigned to N–H in-phase symmetric stretch (ν NH), while that at 1030 cm^{-1} is attributed to C–N stretching vibration (ν CN). The peak observed at 1640 cm^{-1} can either be due to a C═O stretching peak (ν C═O) or NH_2 anti-symmetric bending (δ_{as} NH_2) [51]. The FTIR spectra for the bulk urea is presented in ESI Fig. 4c. and show identical functional groups.

Raman spectrum contains anti-symmetric and symmetric NH_2 vibration bands at 3390 and 3224 cm^{-1} respectively (Fig. 1c.). C═O stretching vibration appears at a wavenumber of 1664 cm^{-1} and a peak at 1160 cm^{-1} ascribed to NH_2 deformation was also observed. A symmetric N–C–N stretch, which is the strongest Raman peak in urea, emerges at 1000 cm^{-1}. A weak Raman band due to N–C–N bending was observed at 500 cm^{-1} [52].

The XRD pattern of urea nanoparticles is represented in Fig. 1d. A comparative pattern of XRD peaks between the bulk technical

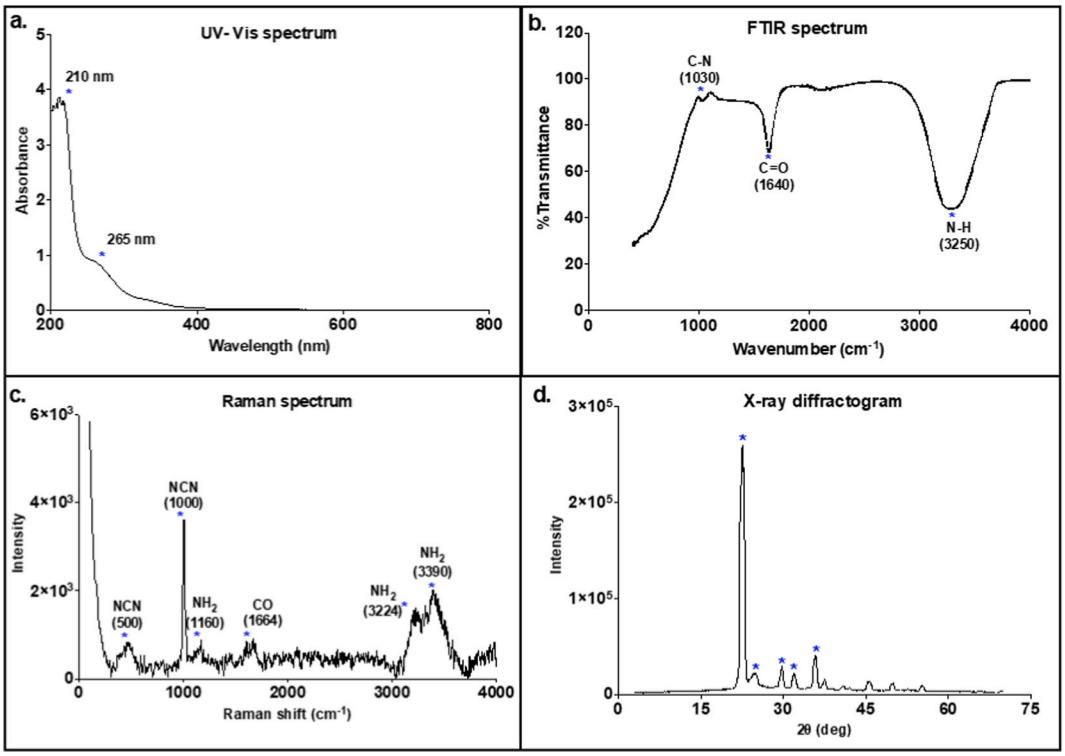

Fig. 1. Characteristic peaks (shown by *) of urea nanoparticles from (a.) UV–Vis spectroscopy at 210 and 265 nm, (b.) FTIR spectroscopy indicating C–N (1030 cm^{-1}), C═O (1640 cm^{-1}) and N–H (3250 cm^{-1}) bonds, (c.) Raman spectroscopy indicating N–C–N (500, 100 cm^{-1}), N–H (1160, 3224 and 3390 cm^{-1}) and C═O (1664 cm^{-1}) bonds and (d.) X-ray diffraction (* = 22.5°, 24.7°, 29.7°, 31.9°, 35.7°) showing characteristic urea peak at 22.5°.

urea (substrate) and TNU is presented in ESI Fig. 4d. The diffraction pattern of synthesised TNU was observed to be comparable with that of bulk urea. As illustrated, the characteristic diffraction peaks of bulk urea and TNU showed similar patterns with the most intense peak at 22.5°. Bulk urea [53] had the 2θ values at 22.5°–22.8°, 25°, 29.5°–29.8°, 32.2°, 36.03°, 37.4°, 42.07°, 50° and 55–55.3°, and TNU had the 2θ values at 22.5°, 24.7°, 29.7°, 31.9°, 35.7°, 37.4°, 42.04°, 49.8° and 55.2°. The minor shifting in the non-prominent peaks of the TNU may occur due to the zero shift of X-Ray diffractometer. The crystallite size was auto-calculated in the instrument from the most intense peak using the Debye – Scherrer formula [54] and was found to be 14.5 nm for TNU whereas, for the bulk urea, the same peak delivered crystallite size as 96.2 nm. It is worth noting here that the peak broadening at 22.5° increases significantly as the crystalline size decreases from 96.2 to 14.5 nm (ESI Fig. 4d.). This peak broadening and drop in intensity confirms the conversion of bulk material (technical urea) to nanoparticles (TNU) [55,56].

The physicochemical characterisation reveals that the TNU retain the inherent characteristics of urea. This strongly supports the TNU can be used an alternative to conventional urea in supplementing nitrogen to plants. The nano-characteristics of TNU will enable its rapid uptake, in-plant localisation, and slow release of nitrogen in plants.

The absolute size and morphology of TNU particles were determined using TEM (Fig. 2a.). It was observed that the particles were spherical shaped and had size in a range of 2.2–45.6 nm with an average size of 12.14 ± 7.79 nm as estimated from the measurement of 200 particles [45]. TNU dispersions were also characterised in serum free cell culture media: incomplete media (ICM) and serum (10 % *v/v* fetal bovine serum) supplemented cell culture media: complete media (CM). The hydrodynamic characteristics in different media are presented in Fig. 2. The Z-average sizes of TNU were 248.05 ± 15.49 nm, 197.57 ± 13.67 nm, and 50.14 ± 11.20 nm respectively for dispersion in DI water (Fig. 2b.), ICM (Fig. 2c.) and CM (Fig. 2d.). The polydispersity indices were 0.405 ± 0.045, 0.348 ± 0.061 and 0.517 ± 0.141 for dispersion in DI water, ICM and CM, respectively. The zeta-potentials were −14.6 ± 0.82 mV, −4.30 ± 1.24 mV, and −9.69 ± 0.8 mV for dispersion in DI water, ICM and CM, respectively. The electrical conductivities were 5.54 ± 0.506 mS/cm, 15.6 ± 0.4 mS/cm and 15.6 ± 0.252 mS/cm for dispersion in DI water, ICM and CM, respectively. The complete cell culture media is a complex system which includes amino acids, proteins, and ionic salts. These media components alter the hydrodynamic behaviour of the nanoparticles [57]. Presence of the proteins around the nanoparticle surface can either further stabilise or de-stabilise the nanoparticles as they either gain or lose surface functionality [58]. From our results it is clear that the TNU particles undergo a hydrodynamic size reduction when suspended in the cell culture media. There is a 1.25 times reduction in the Z-average when the TNU particles are dispersed in the serum free media. On further adding the serum protein components from the fetal bovine serum (FBS), the Z-average size is reduced by 4.95 times. Previous reports have shown that though the serum free media shows affinity to interact with the suspended nanoparticles, FBS has stronger interactions with the nanoparticles in presence of smaller media components such as

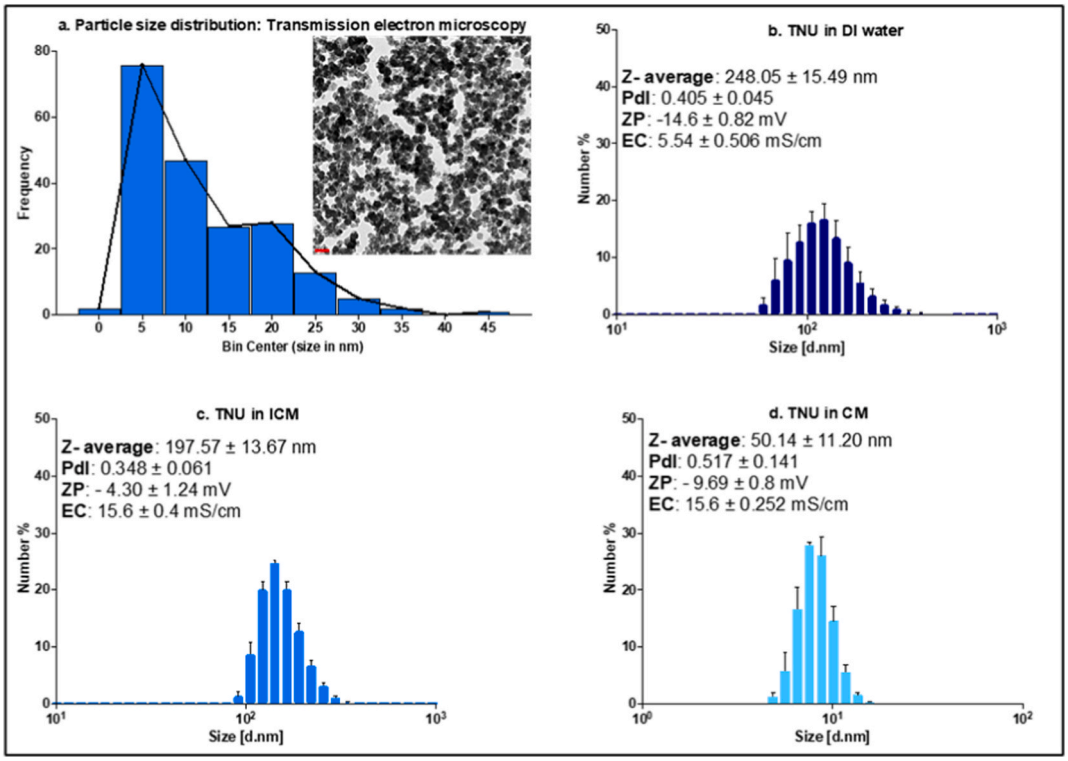

Fig. 2. a. The size distribution of TNU nanoparticles from transmission electron microscopy (inset TEM image at 100 nm scale showing TNU nanoparticles) indicating average size: 12.14 ± 7.79 nm. Hydrodynamic characteristics of urea nanoparticles (TNU) in terms of Z-average size), polydispersity index (PdI), zeta-potential (ZP) and electrical conductivity (EC) in **b.** de-ionised water (DI water) with Z-average: 248.05 ± 15.49 nm, **c.** serum free cell culture media (ICM) with Z-average: 197.57 ± 13.67 nm and **d.** media with serum (CM) with Z-average: 50.14 ± 11.20 nm.

glucose and glutamine [59]. It had been shown for the silver nanoparticles that presence of media components also tends to shift the zetapotential values towards more positive scale after interacting with the nanoparticles [59–62]. Similarly, a study on magnetic iron oxide nanoparticles show that the overall hydrodynamic size is decreased when the nanoparticles interact with the serum supplemented media as compared to serum free media and FBS may act a stabilising factor for colloidal dispersity of the nanoparticles [60]. These interactions between the media components, serum proteins and nanoparticles have shown to influence their overall cytotoxicity. In one of the reports, six different metal oxide nanoparticles based on nickel, zinc, titanium, cerium, silica, and iron were shown to absorb proteins from the FBS and were found to have better cytocompatibility than the bare nanoparticles in human keratinocyte HaCaT cells and human lung carcinoma A549 cells [61]. Another study reports the reduction of hydrodynamic size of titania nanoparticles on interactions with FBS which resulted in higher uptake in human lung cell lines – A549 and H1299 and reduced the cytotoxic effects of the nanoparticles [62]. Our results indicate that in the presence of serum supplemented media, TNU particles have significantly ($p < 0.05$) reduced size for hydrodynamic sphere. This smaller size potentially will result in higher cellular uptake and intracellular interactions.

3.2. *In vitro biocompatibility of biogenic urea nanoparticles (TNU) in WI-38 cells*

The cellular viability was determined by WST-1 assay in human lung fibroblast cells WI-38 at 24, 48 and 72 h from the TNU exposure (Fig. 3a.). At 24 h, the cell viability across all the concentration from 1.5 to 1000 μg/mL was like the untreated control (0 μg/mL). At 48 h, slight decrease in the mitochondrial activity was observed at lower concentrations of exposure with minimal activity of 94.35 ± 7.39 % at 10 μg/mL. At 72 h, decrease in cellular activity was observed with minimal activity of 80.59 ± 5.12 % at 100 μg/mL. No LC_{50} was observed up to 72 h of exposure and 1000 μg/mL concentration (Fig. 3b.). The nanoparticles can easily gain access to the human body through respiratory system and therefore assessment of their direct effects on the non-cancerous lung model system is important. Previously, biocompatibility of green synthesised silver nanoparticles has been shown using WI-38 cells up to a dose of 100 μg/mL and 24 h [63]. On the contrary another study on copper and copper oxide nanoparticles showed cytotoxicity and genotoxicity in WI-38 and A549 cells when tested up to 72 h [64]. It is important to note that given the high surface area to volume ratio of the nanoparticles, the interpretation of the *in vitro* assays based on tetrazolium salt reduction such as WST-1, MTT, MTS needs to be derived by considering the potential assay interference caused due to the nanoparticles [65]. It has been reported that the metallic

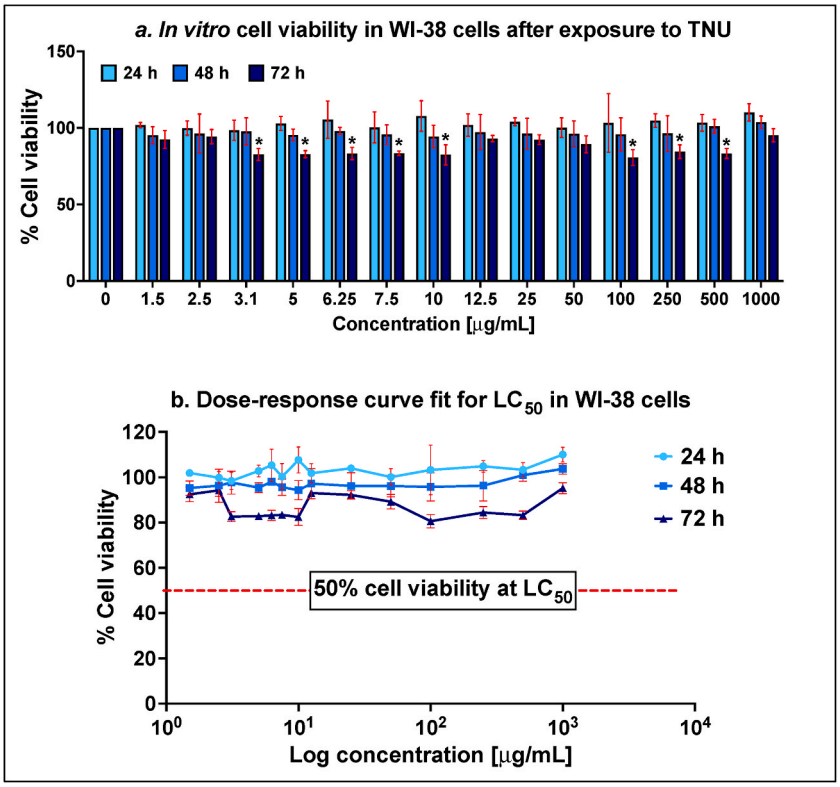

Fig. 3. Effects of different concentrations and exposure time on the cell viability of WI-38 cells after exposure to TNU for 24, 48 and 72 h as determined by WST-1 assay. **a.** Cells were exposed to increasing concentrations of TNU (0, 1.5, 2.5, 3.1, 5, 6.25, 7.5, 10, 12.5, 25, 50, 100, 250, 500, and 1000 μg/mL) and % cell viability is determined with respect to untreated control. b. TNU concentrations were log transformed and asymmetric sigmoidal dose-response curves were fit for LC_{50}. Data is presented as mean ± standard deviation and analysed using ANOVA followed by Dunnett's multiple comparison test. Statistical significance with reference to untreated control is presented by * for $p < 0.05$.

nanoparticles such as those of silver show interfered absorption with the assay components [65], whereas non-metallic nanoparticles such as those of hydroxyapatite tend to adsorb the assay components [66]. This assay interference cannot be eliminated precisely and hence the trend of dose-dependent cellular activity can be indicative of nanoparticle effects on the cells. These *in vitro* results therefore need to be interpreted in parallel with the *in vivo* outcomes.

3.3. Acute effects of biogenic urea nanoparticles (TNU) in New Zealand rabbits

The acute effects of TNU in New Zealand rabbits were evaluated by monitoring the survival, toxic response, and clinical observations up to 21 days from instillation for the three doses: 3.75, 7.5 and 15 μg/mL. After ocular instillation, 100 % survival of New Zealand rabbits up to 21 days was recorded. No toxicity sign was observed in different doses at different time intervals. Additionally, post-instillation, no abnormality was observed in the sensory functions, grip strength and motor activities.

3.4. Sublethal effects of biogenic urea nanoparticles (TNU) in New Zealand rabbits

The sublethal effects of TNU were determined in terms of body weight (Fig. 4.) and occurrence of ocular lesions (Table 1 and Fig. 5.). The body weight of the animals treated with TNU at doses 3.75, 7.5 and 15 μg/mL were similar to the untreated control at day 1 (904.5 ± 10.7 g), day 7 (914.5 ± 11.8 g) and day 21 (933.5 ± 12.1 g) with no significance difference ($p > 0.05$).

No ocular lesions in cornea, iris, and conjunctivae; or chemosis was observed in untreated animals and animals treated with saline 0.9 % (w/v) (Fig. 5a. – b.). At 14th day (Fig. 5c.), only grade 1 lesion in cornea at TNU dose of 3.75 μg/mL was observed with scattered or diffuse areas of opacity but with clearly visible iris, however, this was reversed by day 21 with no further lesions seen at day 21 (Fig. 5f.). For TNU dose of 7.5 μg/mL (Fig. 5d.) grade 1 lesions were observed on the day 14 in cornea (scattered or diffuse areas of opacity), iris (visible deepened rugae, congestion, swelling, moderate circumcorneal hyperaemia and sluggish reaction to light), conjunctivae (some visible blood vessels hyperaemic) and on day 7 for chemosis (some visible swelling above normal). All these ocular lesions were reversed by day 21 (Fig. 5g.). In case of TNU dose of 15 μg/mL, at day 1 grade 1 lesions were observed in conjunctivae with some visible blood vessels hyperaemic and for chemosis with some visible swelling above normal. Interestingly, these lesions got reversed by the day 7–14 (Fig. 5e.) and no further ocular discomfort was observed till day 21 (Fig. 5h.). Similar to our results, some previous studies have also reported reversible minimal eye irritation in rabbits using graphene oxide nanosheets [41], carbon nanotubes [67,68] and fullerenes [69,70].

4. Conclusions

Urea nanoparticles (TNU) were developed biogenically for application as a nitrogen fertiliser. Potential occupational toxicity was systematically assessed for lung and eye tissues by testing the effects of NMs on the cellular mitochondrial dehydrogenase activity in human WI-38 cells, as well as the animal ocular surface irritation in New Zealand rabbits. The results show that the TNU nanoparticles do not cause damage to the cellular mitochondrial activity up to 72 h of exposure and hence the cell viability is not compromised on exposure to TNU nanoparticles. The *in vivo* results show that after exposure to TNU, neither acute inflammation nor corneal epithelial lesions are found. In all the experimental setups, no obvious irreversible irritation or significant chemosis in cornea, iris, or conjunctivae on exposure to TNU was seen. These results show that the biogenic TNU particles have good pulmonary and ocular biocompatibility to the non-target species and hence can be considered as non-hazardous for potential occupational exposure. Considering the global need for effective fertilisers, the use of biogenic urea nanofertilisers will be very crucial for sustainable agriculture. This study on the biocompatibility of urea nanoparticles suggests that as a safe fertiliser, TNU can be employed for the large-scale application to the agricultural fields.

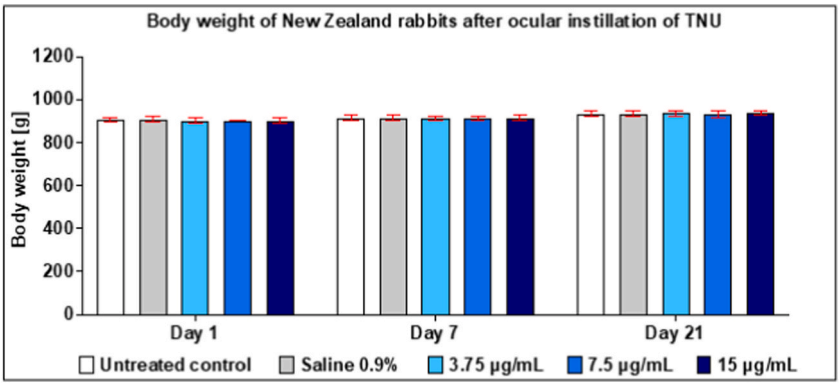

Fig. 4. Body weight of New Zealand rabbits after exposure to TNU at the concentrations of 3.75, 7.5 and 15 μg/mL. Data presented as mean ± standard deviation and analysed using ANOVA followed by Dunnett's multiple comparison test.

Table 1
Grading of ocular lesions in New Zealand rabbits after ocular instillation of TNU and TND.

	Cornea				Iris				Conjunctivae				Chemosis			
	Days				Days				Days				Days			
	1	7	14	21	1	7	14	21	1	7	14	21	1	7	14	21
Untreated control	0	0	0	0	0	0	0	0	0	0	0	0	0	0	0	0
Saline 0.9% (*w/v*)	0	0	0	0	0	0	0	0	0	0	0	0	0	0	0	0
TNU (3.75 μg/mL)	0	0	1	0	0	0	0	0	0	0	0	0	0	0	0	0
TNU (7 μg/mL)	0	0	1	0	0	0	1	0	0	0	1	0	0	1	0	0
TNU (15 μg/mL)	0	0	0	0	0	0	0	0	1	0	0	0	1	0	0	0

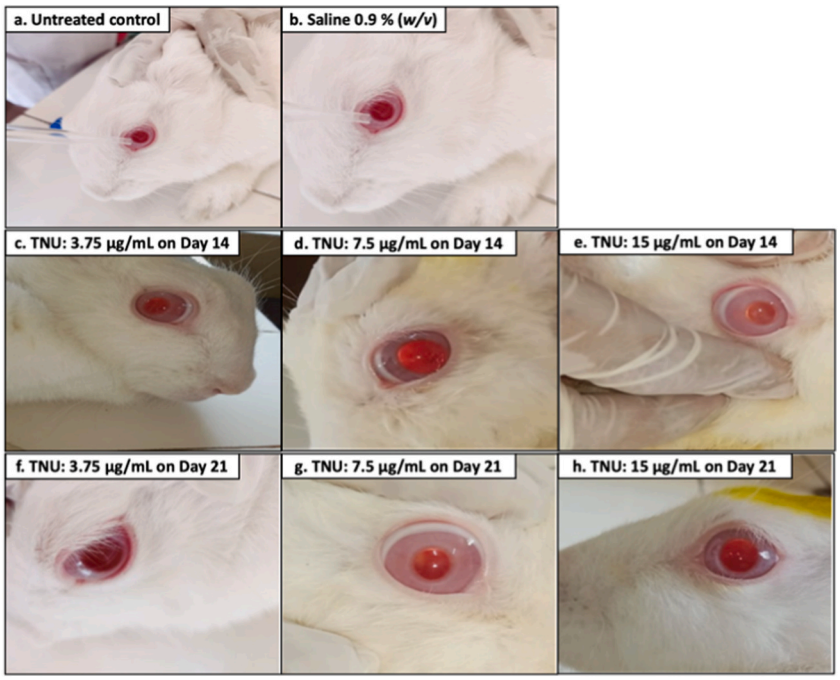

Fig. 5. Representative images of New Zealand rabbits for ocular lesions: in cornea, iris, conjunctivae and for chemosis in the case of (a.) untreated control, (b.) Saline 0.9 % (*w/v*), c. 3.75 μg/mL TNU at day 14, d. 7.5 μg/mL TNU at day 14, e. 15 μg/mL TNU at day 14, f. 3.75 μg/mL TNU at day 21, g. 7.5 μg/mL TNU at day 21 and h. 15 μg/mL TNU at day 21.

Data availability statement

Data included in article/supp. material/referenced in article.

CRediT authorship contribution statement

Ayushi Priyam: Conceptualization, Data curation, Investigation, Methodology, Writing – original draft, Writing – review & editing. **Prerna Seth:** Methodology. **Jibananda Mishra:** Data curation, Investigation, Methodology, Resources, Validation. **Palash Kumar Manna:** Data curation, Investigation, Methodology. **Pushplata Prasad Singh:** Conceptualization, Formal analysis,

Investigation, Methodology, Supervision, Writing – review & editing.

Declaration of competing interest

The authors declare no personal and financial conflict of interest.

Acknowledgment

The research activities of the authors are supported by TERI-Deakin Nanobiotechnology Centre, Gurugram, India, AAL Biosciences Research Pvt. Ltd. Panchkula, Haryana, India and Deakin University, Australia. The authors acknowledge Dr Shruti Shukla (TERI), Mr. Chandrakant Tripathi (TERI) and Ms Prachi Mishra (AAL Biosciences) for their coordination and support.

Appendix A. Supplementary data

Supplementary data to this article can be found online at https://doi.org/10.1016/j.heliyon.2023.e21623.

References

[1] N.L. Ma, et al., Use, exposure and omics characterisation of potential hazard in nanomaterials, Materials Today Advances 17 (2023), 100341.
[2] M. Escribà-Gelonch, et al., Definition of agronomic circular economy metrics and use for assessment for a nanofertilizer case study, Plant Physiol. Biochem. 196 (2023) 917–924.
[3] S.M. El-Bialy, et al., Biological nanofertilizers to enhance growth potential of strawberry seedlings by boosting photosynthetic pigments, plant enzymatic antioxidants, and nutritional status, Plants 12 (2) (2023) 302.
[4] C.-P. Witte, Urea metabolism in plants, Plant Sci. 180 (3) (2011) 431–438.
[5] P. Zhang, et al., Nanotechnology and artificial intelligence to enable sustainable and precision agriculture, Nat. Plants 7 (7) (2021) 864–876.
[6] Y. Kumar, et al., Nanofertilizers and their role in sustainable agriculture, Annals of Plant and Soil Research 23 (3) (2021) 238–255.
[7] M.H. Rahman, K.S. Haque, M.Z.H. Khan, A review on application of controlled released fertilizers influencing the sustainable agricultural production: a Cleaner production process, Environmental Technology & Innovation 23 (2021), 101697.
[8] R. Kumar, et al., Nano urea: an efficient tool for precision agriculture and sustainability, Vigyan Varta 2 (9) (2021) 72–74.
[9] S. Sharma, et al., Nanotechnology: a modern approach of crop improvement in agricultural crops. https://www.krishisewa.com/production-technology/1509-nanotechnology-a-modern-approach-of-crop-improvement-in-agricultural-crops.html, 2023.
[10] P.P. Singh, et al., Biologically synthesised urea-based nanomaterial shows enhanced agronomic benefits in maize and rice crops during Kharif season, Sci. Hortic. 315 (2023), 111988.
[11] K.B. Narayanan, N. Sakthivel, Biological synthesis of metal nanoparticles by microbes, Adv. Colloid Interface Sci. 156 (1–2) (2010) 1–13.
[12] S.H. Sadeghi, L. Moradi, Solvent free synthesis of amidoalkyl derivatives under green and convenient conditions, J. Heterocycl. Chem. 59 (4) (2022) 695–703.
[13] N.C. Sharma, et al., Synthesis of plant-mediated gold nanoparticles and catalytic role of biomatrix-embedded nanomaterials, Environ. Sci. Technol. 41 (14) (2007) 5137–5142.
[14] S. Selvinsimpson, Y. Chen, Microbial-based synthesis of nanoparticles to remove different pollutants from wastewater, in: Environmental Applications of Microbial Nanotechnology, Elsevier, 2023, pp. 167–181.
[15] P. Prema, et al., Microbial synthesis of silver nanoparticles using Lactobacillus plantarum for antioxidant, antibacterial activities, Inorg. Chem. Commun. 136 (2022), 109139.
[16] E.Z. Gomaa, Microbial mediated synthesis of zinc oxide nanoparticles, characterization and multifaceted applications, J. Inorg. Organomet. Polym. Mater. 32 (11) (2022) 4114–4132.
[17] I.I. Alao, et al., Green synthesis of copper nanoparticles and investigation of its anti-microbial properties, Advanced Journal of Chemistry-Section B 4 (1) (2022) 39–52.
[18] A. Bedi, et al., An Aspergillus aculateus strain was capable of producing agriculturally useful nanoparticles via bioremediation of iron ore tailings, J. Environ. Manag. 215 (2018) 100–107.
[19] A. Bedi, B.R. Singh, Microcosm based bio-efficacy evaluation of biologically produced nano-Zn–Fe fertiliser, Adv. Nat. Sci. Nanosci. Nanotechnol. 13 (2) (2022), 025010.
[20] A. Priyam, et al., A new method for biological synthesis of agriculturally relevant nanohydroxyapatite with elucidated effects on soil bacteria, Sci. Rep. 9 (1) (2019), 15083.
[21] A. Hasanzadeh, et al., Biosynthesis of AgNPs onto the urea-based periodic mesoporous organosilica (AgxNPs/Ur-PMO) for antibacterial and cell viability assay, J. Colloid Interface Sci. 585 (2021) 676–683.
[22] A. Adewuyi, et al., Use of Urea-imprinted cobalt ferrite nanoparticles in deacidification of deteriorated vegetable oil: synthesis, characterization and preclinical toxicity screening, J. Mol. Liq. 365 (2022), 120224.
[23] S. Ghasempour, et al., The acute toxicity of urea coated ferrous oxide nanoparticles on L929 cell line, evaluation of biochemical and pathological parameters in rat kidney and liver, Physiology and Pharmacology 17 (4) (2014) 423–436.
[24] A. Adholeya, R. Singh, Guidelines for Evaluation of Nano-Based Agri-Input & Food Products in India, 2020.
[25] A. Rafieepour, M. R Azari, F. Khodagholi, Cytotoxic effects of crystalline silica in form of micro and nanoparticles on the human lung cell line A549, Toxicol. Ind. Health 39 (1) (2023) 23–35.
[26] B. Wu, et al., Combined effects of graphene oxide and zinc oxide nanoparticle on human A549 cells: bioavailability, toxicity and mechanisms, Environ. Sci.: Nano 6 (2) (2019) 635–645.
[27] L. Bobyk, et al., Toxicity and chemical transformation of silver nanoparticles in A549 lung cells: dose-rate-dependent genotoxic impact, Environ. Sci.: Nano 8 (3) (2021) 806–821.
[28] E. Moschini, et al., Biological mechanism of cell oxidative stress and death during short-term exposure to nano CuO, Sci. Rep. 13 (1) (2023) 2326.
[29] C. Dong, et al., Assessment of the pulmonary toxic potential of nano-tobacco stem-pyrolyzed biochars, Environ. Sci.: Nano 6 (5) (2019) 1527–1535.
[30] B.M. Strauch, W. Hubele, A. Hartwig, Impact of endocytosis and lysosomal acidification on the toxicity of copper oxide nano-and microsized particles: uptake and gene expression related to oxidative stress and the DNA damage response, Nanomaterials 10 (4) (2020) 679.
[31] Y. Zhang, et al., MMP-3 activation is involved in copper oxide nanoparticle-induced epithelial-mesenchymal transition in human lung epithelial cells, Nanotoxicology 15 (10) (2021) 1380–1402.
[32] Y. Zhang, et al., Differences in the characteristics and pulmonary toxicity of nano-and micron-sized respirable coal dust, Respir. Res. 23 (1) (2022) 1–18.

[33] Y. Mo, et al., Nickel nanoparticle-induced cell transformation: involvement of DNA damage and DNA repair defect through HIF-1α/miR-210/Rad52 pathway, J. Nanobiotechnol. 19 (2021) 1–20.
[34] B. Liu, et al., A targeted nano drug delivery system of AS1411 functionalized graphene oxide based composites, ChemistryOpen 10 (4) (2021) 408–413.
[35] A. Amr, D.E. El-Ghwas, Anti-breast Cancer and Cytotoxicity of Nano Materials Formed Bacterial Cellulose-ZnO-Ag Composite, 2022.
[36] M. Stępnik, et al., Cytotoxic effects in 3T3-L1 mouse and WI-38 human fibroblasts following 72 hour and 7 day exposures to commercial silica nanoparticles, Toxicol. Appl. Pharmacol. 263 (1) (2012) 89–101.
[37] V. Kumar, et al., Biocompatible silver nanoparticles from vegetable waste: its characterization and bio-efficacy, Int J Nano Matl Sci 4 (1) (2015) 70–86.
[38] H.Y. Park, D.D. Sin, Stress-induced premature senescence: another mechanism involved in the process of accelerated aging in chronic obstructive pulmonary disease, in: Inflammation, Advancing Age and Nutrition, Elsevier, 2014, pp. 193–202.
[39] OECD, Test No. 405: *Acute Eye Irritation/Corrosion*, OECD Publishing Paris, 2002.
[40] A. Leonardi, et al., Cationic solid lipid nanoparticles enhance ocular hypotensive effect of melatonin in rabbit, International journal of pharmaceutics 478 (1) (2015) 180–186.
[41] W. Wu, et al., Evaluation of the toxicity of graphene oxide exposure to the eye, Nanotoxicology 10 (9) (2016) 1329–1340.
[42] W. An, et al., Ocular toxicity of reduced graphene oxide or graphene oxide exposure in mouse eyes, Exp. Eye Res. 174 (2018) 59–69.
[43] T.W. Prow, et al., Ocular nanoparticle toxicity and transfection of the retina and retinal pigment epithelium, Nanomed. Nanotechnol. Biol. Med. 4 (4) (2008) 340.
[44] V. Hackley, J. Clogston, Measuring the Size of Nanoparticles in Aqueous Media Using Batch-Mode Dynamic Light Scattering, vol. 1200, NIST special publication, 2007, 6.
[45] J.E. Bonevich, W.K. Haller, Measuring the Size of Nanoparticles Using Transmission Electron Microscopy (TEM), 2010.
[46] A.V. Peskin, C.C. Winterbourn, Assay of superoxide dismutase activity in a plate assay using WST-1, Free Radic. Biol. Med. 103 (2017) 188–191.
[47] A. Priyam, et al., Hemocompatibility of biogenic phosphorus nano-agromaterials at environmentally relevant and supra-environmental concentrations for occupational exposure, Environ. Sci. J. Integr. Environ. Res.: Advances 2 (2) (2023) 313–324.
[48] A. Priyam, et al., Multi-endpoint assessments for in vitro nano-bio interactions and uptake of biogenic phosphorus nanomaterials using HEK293 cells, Environ. Sci. J. Integr. Environ. Res.: Advances 2 (5) (2023) 749–766.
[49] H. Bahrulolum, et al., Green synthesis of metal nanoparticles using microorganisms and their application in the agrifood sector, J. Nanobiotechnol. 19 (1) (2021) 1–26.
[50] G. Caldow, J.N. Murrell, The Theory of the Electronic Spectra of Organic Molecules, Chapman and Hall Ltd, Elsevier, London, 1971. XIV+ 328 pages,£ 3.50. 1971.
[51] J. Grdadolnik, Y. Maréchal, Urea and urea–water solutions—an infrared study, J. Mol. Struct. 615 (1–3) (2002) 177–189.
[52] R.L. Frost, et al., Raman spectroscopy of urea and urea-intercalated kaolinites at 77 K, Spectrochim. Acta Mol. Biomol. Spectrosc. 56 (9) (2000) 1681–1691.
[53] C. Tarafder, et al., Formulation of a hybrid nanofertilizer for slow and sustainable release of micronutrients, ACS Omega 5 (37) (2020) 23960–23966.
[54] U. Holzwarth, N. Gibson, The Scherrer equation versus the'Debye-Scherrer equation', Nat. Nanotechnol. 6 (9) (2011), 534-534.
[55] C.F. Holder, R.E. Schaak, Tutorial on Powder X-Ray Diffraction for Characterizing Nanoscale Materials, ACS Publications, 2019, pp. 7359–7365.
[56] S. Mourdikoudis, R.M. Pallares, N.T. Thanh, Characterization techniques for nanoparticles: comparison and complementarity upon studying nanoparticle properties, Nanoscale 10 (27) (2018) 12871–12934.
[57] A. Priyam, et al., Multi-endpoint assessments for in vitro nano-bio interactions and uptake of biogenic phosphorus nanomaterials using HEK293 cells, Environ. Sci. J. Integr. Environ. Res.: Advances (2023).
[58] T.L. Moore, et al., Nanoparticle colloidal stability in cell culture media and impact on cellular interactions, Chem. Soc. Rev. 44 (17) (2015) 6287–6305.
[59] P. Bélteky, et al., Are smaller nanoparticles always better? Understanding the biological effect of size-dependent silver nanoparticle aggregation under biorelevant conditions, Int. J. Nanomed. 16 (2021) 3021.
[60] H.T. Wiogo, et al., Stabilization of magnetic iron oxide nanoparticles in biological media by fetal bovine serum (FBS), Langmuir 27 (2) (2011) 843–850.
[61] M. Horie, et al., Protein adsorption of ultrafine metal oxide and its influence on cytotoxicity toward cultured cells, Chem. Res. Toxicol. 22 (3) (2009) 543–553.
[62] R. Tedja, et al., Effects of serum adsorption on cellular uptake profile and consequent impact of titanium dioxide nanoparticles on human lung cell lines, ACS Nano 6 (5) (2012) 4083–4093.
[63] P. Subramanian, et al., Synthesis of Oldenlandia umbellata stabilized silver nanoparticles and their antioxidant effect, antibacterial activity, and bio-compatibility using human lung fibroblast cell line WI-38, Process Biochem. 86 (2019) 196–204.
[64] H.M. Fahmy, N.M. Ebrahim, M.H. Gaber, In-vitro evaluation of copper/copper oxide nanoparticles cytotoxicity and genotoxicity in normal and cancer lung cell lines, J. Trace Elem. Med. Biol. 60 (2020), 126481.
[65] D.F. Mello, et al., Caveats to the use of MTT, neutral red, Hoechst and Resazurin to measure silver nanoparticle cytotoxicity, Chem. Biol. Interact. 315 (2020), 108868.
[66] C. Santos, et al., Vascular biosafety of commercial hydroxyapatite particles: discrepancy between blood compatibility assays and endothelial cell behavior, J. Nanobiotechnol. 16 (1) (2018) 1–15.
[67] M. Ema, et al., Evaluation of dermal and eye irritation and skin sensitization due to carbon nanotubes, Regul. Toxicol. Pharmacol. 61 (3) (2011) 276–281.
[68] A.S. Kishore, P. Surekha, P.B. Murthy, Assessment of the dermal and ocular irritation potential of multi-walled carbon nanotubes by using in vitro and in vivo methods, Toxicology letters 191 (2–3) (2009) 268–274.
[69] M. Ema, et al., Dermal and ocular irritation and skin sensitization studies of fullerene C60 nanoparticles, Cutan. Ocul. Toxicol. 32 (2) (2013) 128–134.
[70] H. Aoshima, et al., Safety evaluation of highly purified fullerenes (HPFs): based on screening of eye and skin damage, J. Toxicol. Sci. 34 (5) (2009) 555–562.